

# Green Chemistry

Cutting-edge research for a greener sustainable future

[rsc.li/greenchem](https://rsc.li/greenchem)



ISSN 1463-9262

**PAPER**

Robert Wojcieszak, Ivaldo Itabaiana *et al.*  
Optimization of 5-hydroxymethylfurfural oxidation via  
photo-enzymatic cascade process





Cite this: *Green Chem.*, 2024, **26**, 8211

## Optimization of 5-hydroxymethylfurfural oxidation via photo-enzymatic cascade process†

Marcelo A. do Nascimento,<sup>a,b</sup> Bernardo Haber,<sup>a</sup> Mauro R. B. P. Gomez,<sup>a</sup> Raquel A. C. Leão,<sup>a</sup> Mariusz Pietrowski,<sup>c</sup> Michał Zieliński,<sup>c</sup> Rodrigo O. M. A. de Souza,<sup>a</sup> Robert Wojcieszak<sup>a,b,d</sup> and Ivaldo Itabaiana, Jr.<sup>\*b,e</sup>

This study investigated the oxidation of 5-hydroxymethylfurfural (HMF) to produce valuable products such as 2,5-furandicarboxaldehyde (DFF), 5-formyl-2-furancarboxylic acid (FFCA) and 2,5-furandicarboxylic acid (FDCA) through (photo) chemical and enzymatic catalysis. Laccases from different sources, including *Aspergillus* spp., *Pseudomonas cepacea*, and *Trametes versicolor*, were evaluated for their catalytic activity in the HMF oxidation. Laccase from *Trametes versicolor* (LacTV) emerged as the most effective catalyst, achieving complete conversion of HMF under specific pH conditions. The reaction mechanisms were explored, revealing a preference for the primary alcohol oxidation pathway over the aldehyde, leading to the formation of DFF and subsequent conversion to FFCA and FDCA. The impact of substrate concentration on HMF conversion was examined, revealing optimal conversion at lower HMF concentrations (<100 mM) and reduced performance at higher concentrations (>100 mM). The study also examined the influence of blue light (430 nm) on this reaction, revealing the dependence on light exposure for gC<sub>3</sub>N<sub>4</sub> based catalysts and a negative effect for LacTV. Furthermore, the study introduces a modular flow chemical platform that utilizes Continuous Stirred Tank Reactors (CSTR) in a cascade configuration, the optimization of HMF oxidation. The implementation of this innovative approach has led to the effective synthesis of FDCA, demonstrating an impressive 40-fold increase in productivity compared to the traditional batch system. These results present significant potential for advancing green chemistry and sustainable chemical synthesis, introducing novel possibilities for environmentally friendly HMF oxidation processes.

Received 5th February 2024,

Accepted 8th April 2024

DOI: 10.1039/d4gc00673a

[rsc.li/greenchem](http://rsc.li/greenchem)

## Introduction

Developing sustainable and environmentally friendly chemical processes is paramount in contemporary research. Among the diverse platforms for sustainable chemical synthesis, 5-hydroxymethylfurfural (HMF) is one strategic chemical compound that has attracted increasing attention in the last ten years.<sup>1,2</sup> HMF, a biobased compound derived from renewable resources via dehydration of carbohydrates such as levoglucosan,<sup>3</sup> has been listed as one of the top-12 value-added chemi-

cals produced from sustainable bio-substances by the United States Department of Energy.<sup>4</sup> It is widely known as “the sleeping giant”<sup>5</sup> with the potential to be used as a commodity chemical due to the vast industrial application of its derivatives through enzymatic or chemical transformations.<sup>6</sup> Oxidation of HMF provides several value-added chemicals such as 2,5-diformylfuran (DFF), 5-hydroxymethyl-2-furancarboxylic acid (HMFCA), 5-formyl-2-furancarboxylic acid (FFCA), 2,5-furandicarboxylic acid (FDCA). These oxidized derivatives of HMF are applied as a building block in drugs, monomers for synthesizing polymers,<sup>7,8</sup> and polymers, among other furan-based products (Fig. 1).<sup>2,9–11</sup>

Several conventional chemical methods have been employed to oxidize HMF using various chemical catalysts.<sup>12,13</sup> Nowadays, the use of enzymatic catalysis for the selective oxidation of HMF has garnered significant interest due to its ability to provide remarkable regio- or stereoselectivity, effectively address environmental pollution concerns, and offer an ecologically sustainable reaction system.<sup>14</sup> Therefore, laccases deserve special attention. Their natural substrates are the phenolic residues of wood lignin, including suitable mediators, even in catalytic quantities, which enable the oxidation of non-

<sup>a</sup>BOSS Group - Biocatalysis and Organic Synthesis Group, Chemistry Institute, Federal University of Rio de Janeiro, Brazil

<sup>b</sup>Univ. Lille, CNRS, Centrale Lille, Univ. Artois, UMR 8181 - UCCS - Unité de Catalyse et Chimie du Solide, Lille, France. E-mail: Robert.wojcieszak@cnrs.fr, ivaldoufrj@gmail.com

<sup>c</sup>Faculty of Chemistry, Adam Mickiewicz University, Poznań, Uniwersytetu Poznańskiego 8, 61-614 Poznań, Poland

<sup>d</sup>Université de Lorraine, CNRS, L2CM UMR 7053, F-54000 Nancy, France

<sup>e</sup>Department of Biochemical Engineering, School of Chemistry, Federal University of Rio de Janeiro, Brazil

† Electronic supplementary information (ESI) available. See DOI: <https://doi.org/10.1039/d4gc00673a>

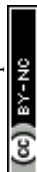




**Fig. 1** HMF and value-added oxidized derivatives. 2,5-diformylfuran (DFF), 5-hydroxymethyl-2-furancarboxylic acid (HMFA), 5-formyl-2-furancarboxylic acid (FFCA), 2,5-furandicarboxylic acid (FDCA) and 5-hydroxymethylfurfural (HMF).

phenolic substrates by this enzyme.<sup>14–16</sup> Laccases are enzymes belonging to the multicopper oxidase family that catalyze the oxidation of a wide range of substrates, including phenols, aromatic amines, and aliphatic amines, effectively reducing molecular oxygen to water.<sup>17</sup> It is widely distributed in nature and found in bacteria, fungi, higher plants, and insects.<sup>17,18</sup>

The pioneering study on the biotransformation of HMF was conducted by Koopman *et al.* They investigated the conversion of HMF to FDCA using a fed-batch fermentation approach. Using recombinant *Pseudomonas putida* S12, engineered with the *hmfH* gene encoding an oxidoreductase, they achieved a 97% FDCA yield within 144 h.<sup>19</sup> This study highlighted the significance of the *hmfH* gene in facilitating the successful conversion process.

The biocatalytic conversion of HMF to FFCA was proposed by Krystof *et al.* They conducted extensive investigations exploring various strategies to achieve the selective oxidation of HMF, explicitly focusing on utilizing a catalytic system comprising lipase B from *Candida antarctica* (CaLB) and TEMPO for the oxidation of HMF. Through this innovative CaLB-mediated oxidation process, they successfully achieved an FFCA yield of 52% within a 24-hour timeframe in a *t*-butanol system.<sup>20</sup> Carro *et al.* investigated the capacity of fungal aryl alcohol oxidase (AAO) to oxidize HMF. The findings revealed a high efficiency in the partial oxidation of HMF to FFCA, resulting in a yield of 98% after 4 h.<sup>21</sup> In addition, Dijkman and Fraaije employed the HMF oxidase *Methylovorus sp.* MP688 for the synthesis of FFCA. They achieved an impressive yield of 92% for FFCA after 5 hours of the HMF oxidation process.<sup>22</sup>

In this context, this research investigated the dynamics of HMF oxidation, focusing on optimizing the process and elucidating the underlying mechanisms. Two main approaches are explored: enzymatic catalysis using laccases and photocatalytic oxidation. Laccases, versatile metalloenzymes, have exhibited remarkable potential in mediating the selective oxidation of HMF, offering a greener and more sustainable route to chemical transformation. In parallel, photocatalytic reactions involving innovative catalysts such as graphitic carbon nitride ( $g\text{-C}_3\text{N}_4$  and  $1\% \text{Pd}/g\text{-C}_3\text{N}_4$ ) promise efficient and environmentally benign HMF oxidation.

$g\text{-C}_3\text{N}_4$  is a polymeric semiconductor that can be obtained by thermal condensation of nitrogen-rich precursors such as

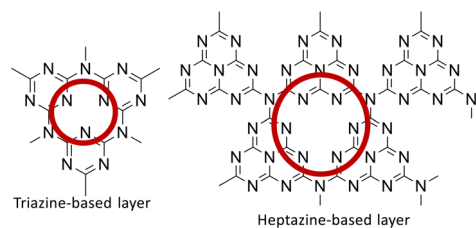


**Fig. 2** Triazine and heptazine-based layer structure  $g\text{-C}_3\text{N}_4$ .

cyanamide, dicyandiamide, melamine, urea, thiourea, and ammonium thiocyanate (Fig. 2).<sup>23</sup>

It stands out as an exceptionally active photocatalyst. The framework topology of the linear polymer “melon” is presumed to consist of interconnected tri-s-triazines *via* secondary nitrogen, while defect-rich  $\text{C}_3\text{N}_4$  takes the form of p-conjugated planar 2D sheets of poly(tri-s-triazines) interconnected *via* tertiary amines. Efforts to enhance the separation/transfer efficiency of photogenerated electron–hole pairs in  $g\text{-C}_3\text{N}_4$  based photocatalysts involve strategies like doping the  $\text{C}_3\text{N}_4$  structure with metals, modifying the synthesis method, performing post-treatments, controlling defects, and combining it with other structures. Among recent strategies,  $g\text{-C}_3\text{N}_4$  based heterostructures show promise due to their ability to spatially separate photogenerated electron–hole pairs, suppressing recombination. The rational design of  $g\text{-C}_3\text{N}_4$  based heterostructures holds potential for creating highly efficient visible-light-driven photocatalysts with applications in chemical synthesis, environmental remediation, and energy-related processes.

In this work we used a modular flow chemistry platform through continuous stirred tank reactors (CSTR) in cascade configuration to optimize HMF oxidation and maximize FDCA production *via* enzymatic and photocatalytic processes. In summary, this research contributes to the growing knowledge of more sustainable chemical synthesis. It offers insights into the efficient production of valuable chemicals from renewable resources, with implications for various industries and applications.

## Results and discussion

### Screening of laccases

The HMF oxidation reaction was initially used as a model in the screening performed with laccases from *Aspergillus* spp. (*LacAsp*), *Pseudomonas cepacea* (*LacPC*), and *Trametes versicolor* (*LacTV*), which exhibited different activities in the oxidation of ABTS ( $44 \text{ U mg}^{-1}$ ,  $2.7 \text{ U mg}^{-1}$ , and  $1.88 \text{ U mg}^{-1}$ , respectively). Therefore, 5 U of activity of each free enzyme was used to oxidize 25 mM HMF at pH 4.5, pH 6.0, and pH 7.0 in a Laccase–Mediator–Substrate (LMS) system. TEMPO was a constant mediator in all conditions (Table 1).<sup>24</sup>

As shown in Table 1, better results were obtained for *LacTV* with 100% conversion at pH 4.5 and pH 6.0 (entries 8 and 9),



**Table 1** Initial screening of laccases through HMF oxidation at pH 7.0, 6.0, and 4.5

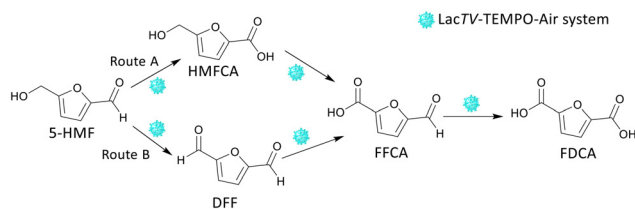
Entry	Enzyme <sup>a</sup>	pH <sup>b</sup>	Conversion (%)
1	LacAsp	7.0	8
2		6.0	11
3		4.5	14
4	LacPC	7.0	7
5		6.0	4
6		4.5	0
7	LacTV	7.0	51
8		6.0	100
9		4.5	100
10	—	7.0	0
11	—	6.0	0
12	—	4.5	0

<sup>a</sup> Reaction condition: free laccases (5U) from *Trametes versicolor* (LacTV), *Aspergillus* spp. (LacAsp) and *Pseudomonas cepacea* (LacPC), respectively. <sup>b</sup> Phosphate buffer pH 7.0 (50 mM), citrate buffer pH 6.0 (50 mM), and acetate buffer pH 4.5 (50 mM); HMF (25 mM), TEMPO (0.3 eq.), reaction time 96 h at 30 °C and 300 rpm. The control experiment carried out without enzyme at different pH (4.5; 6.0 and 7.0), mediator TEMPO (0.3 eq.) and HMF (25 mM) (entries: 10–12).

compared to 51% at pH 7.0 (entry 7). LacPC and LacAsp exhibited similar conversions at pH 7.0 (entries 1 and 4), while at pH 4.5, LacAsp led to low conversions (entry 3), and no conversions were observed to LacPC (entry 6). Similar findings were reported by Cascelli *et al.* in the selective oxidation of furfuryl alcohol to furfural using mediators in the presence of LacTV at pH 4.5<sup>25</sup> and Cheng *et al.* in the oxidation of HMF using TEMPO as a mediator in the presence of LacTV at pH 4.5 and 6.0.<sup>26</sup>

From these preliminary results, it was found that the pH strongly influences the rate of the reaction. The LacTV could oxidize HMF to FFCA in acetate buffer (50 mM, pH 4.5), and in the presence of citrate buffer (50 mM, pH 6.0), FDCA was the main product. According to Bassanini *et al.* LacTV has emerged as one of the most widely used laccases for the oxidation of primary and secondary alcohols, facilitating the conversion of these alcohols into their respective carbonyl compound.<sup>27</sup> HMF has both an aldehyde group and an alcohol group, and the transformation of HMF to FDCA involves three successive oxidation steps *via* route A or B (Fig. 3).

To produce FDCA from HMF, the LacTV must act on the hydroxymethyl and aldehyde groups. The study of the reaction mechanism proposed by Dijkman *et al.* suggested that the oxidase targets alcohol groups and relies on aldehyde hydration for the oxidation step essential to produce FDCA.<sup>28</sup> Furthermore, Yang *et al.* reported that HMF could undergo oxidation to produce FFCA and FDCA when exposed to the laccase-TEMPO system in a phosphate buffer (200 mM, pH 6).<sup>29</sup> This observation was attributed to the high presence of

**Fig. 3** Pathway for the conversion of 5-hydroxymethylfurfural (HMF) to 2,5-furan dicarboxylic acid (FDCA): route A: HMF to 5-hydroxymethyl-2-furancarboxylic acid (HMFA), HMFA to 2,5-formylfuran-3-carboxylic acid (FFCA) and FFCA to FDCA. Route B: HMF to DFF, DFF to FFCA, and FFCA to FDCA.

the hydrated form of FFCA (Gem-Diol) due to the promoting effect of buffer salts like phosphate on aldehyde hydration.<sup>30,31</sup> In this context, FDCA synthesis was optimized using the best conditions found in this initial screening: LacTV in acetate buffer (pH 4.5) and citrate (pH 6.0).

### Influence of buffer composition and ionic strength on HMF oxidation

Fig. 4 shows the influence of buffer composition and ionic strength on the oxidation of HMF catalyzed by the LacTV-TEMPO system. The use of acetate buffer promoted the production of FFCA. Furthermore, the results suggest that under these conditions, the increase in ionic strength did not favor the oxidation of HMF, leading to a 19% reduction in conversion (from 25 mM to 100 mM, pH 4.5). On the contrary, it was also possible to observe the formation of DFF (11% at 100 mM), which was not observed at 25- and 50 mM ionic strengths, respectively. Consequently, the selectivity to FDCA decreased (<35%). Notably, the formation of HMFA was not observed in either of the conditions investigated. Anions exhibit a remarkable ability to interact with proteins, disrupting their structural integrity through hydrogen bonding and Coulomb interactions.<sup>32</sup> These interactions, influenced by anion size, can induce conformational changes in enzymes, potentially deactivating or enhancing their activity. The impact

**Fig. 4** Effect of buffer (acetate pH 4.5 and citrate pH 6.0) and ionic strength (25, 50, 75, and 100 mM, respectively) in the selectivity and conversion on the oxidation of HMF by LacTV-TEMPO system. Reaction condition: HMF (25 mM), TEMPO (0.3 equivalents), LacTV (5 U), reaction time (48 h), 30 °C and 300 rpm.

of anions on enzyme function varies depending on their interaction with active sites; competitive inhibition may hinder substrate binding, while non-competitive inhibition affects sites distal to the active site.<sup>33</sup> For instance, Steven *et al.*<sup>34</sup> demonstrated how acetate anions competitively inhibit laccase activity by obstructing the binding of ABTS (2,2 Azino bis-(3-ethylbenzo thiazoline-6 sulfonic acid) diammonium salt) to the active site, thereby impeding electron transfer and enzyme-substrate interaction, especially at higher acetate concentrations. This process may also have occurred at higher concentrations of acetate anions, resulting in a decrease in LacTV activity, as illustrated in Fig. 4.

On the other hand, FDCA formation significantly increased when a citrate buffer was used. Particularly when higher ionic strength was used ( $\geq 50$  mM), the FDCA formation remained constant, as depicted in Fig. 4. Hence, in the presence of a citrate buffer ( $\geq 50$  mM), FDCA can be generated from HMF with complete conversion and a selectivity higher than 68%, findings close to previously reported by Cheng *et al.* with 56% yield for FDCA in citrate buffer (50 mM, pH 6.0) and FFCA yield  $>90\%$  in acetate buffer.<sup>26</sup> These results show a significant influence of buffer composition, pH range, and salt concentration on the HMF oxidation steps catalyzed by the LacTV-TEMPO system.

The mechanism of alcohol oxidation by laccase, utilizing TEMPO as a mediator, was originally proposed by Fabbrini *et al.* Initially, an ionic oxidation mechanism was proposed, wherein laccase, with a redox potential ranging from 0.4 to 0.9 V, readily oxidizes the stable form of the TEMPO oxyl radical to the oxoammonium ion (with a redox potential of  $E^\circ$  0.2 V) (Fig. 5).<sup>35</sup>

Following the initial oxidation, a subsequent step involves the nucleophilic attack of the oxygen lone pair from the HMF substrate onto the TEMPO-oxoammonium, forming an adduct. This transitional adduct undergoes deprotonation at the  $\alpha$ -C-H bond, leading to the generation of the carbonyl product, converting HMF into DFF. Concurrently, the TEMPO molecule is reduced to its hydroxylamine form (R-N-OH). Finally, in the catalytic cycle, the enzyme is oxidized by molecular oxygen (dioxygen), effectively concluding the entire process.<sup>14,35</sup> DFF interacts with water to generate a Gem-Diol species and form other oxidation products. This Gem-Diol undergoes a subsequent nucleophilic attack onto the oxoammonium form of

TEMPO, forming another transient adduct. This adduct is then deprotonated, leading to the production of the desired product, FFCA. Similarly, the conversion of FFCA to FDCA follows a similar mechanism involving the formation of a transient adduct through a nucleophilic attack of the Gem-Diol onto the oxoammonium form of TEMPO, followed by deprotonation. Thus, these results indicate that the preferential path for the oxidation of HMF by the LacTV-TEMPO system occurs *via* route B (Fig. 3). First, oxidation of the primary alcohol to aldehyde, producing DFF, followed by oxidation of the aldehyde group to form FFCA and subsequently converted into FDCA by oxidation of the second aldehyde group.

### Effect of the HMF concentration

Based on the preliminary results discussed above, the effect of the HMF concentration (25–300 mM) on the performance of the LacTV-TEMPO system was also investigated. Citrate buffer (75 mM, pH 6.0) was selected for this study. Fig. 6a and b shows the effect of HMF concentration on conversion and FDCA yield. It was found that HMF was fully converted after 48 h in the concentration range (25–100 mM), resulting in the highest FDCA yield of 51% obtained at HMF concentration (75 mM). This is lower than the 83% reported in citrate buffer (300 mM, pH 6.0). However, in our case lower ionic strength (75 mM) and low enzyme load ( $0.5 \text{ mg mL}^{-1}$ ) compared to reported ( $1.0 \text{ mg mL}^{-1}$ ).<sup>26</sup> Furthermore, as expected a significant reduction in conversion was found at higher HMF concentrations (300 mM).

### Influence of blue light (460 nm) on HMF oxidation *via* hybrid photocatalytic ( $\text{gC}_3\text{N}_4$ and $1\% \text{Pd/gC}_3\text{N}_4$ ) and enzymatic (LacTV) processes

Based on previous works,<sup>7,36–38</sup> a study was conducted to assess the photocatalytic potential of  $\text{gC}_3\text{N}_4$  and  $1\% \text{Pd/gC}_3\text{N}_4$  in the oxidation of HMF. The characterization of this catalyst is presented in ESI (Fig. S1, S2 and S3†). This investigation encompassed both the presence and absence of blue light and the TEMPO mediator, exploring the light-LacTV interaction during a total reaction time of 48 hours under the optimized conditions in this study, which included pH (6.0), ionic strength (75 mM), and HMF concentration (75 mM). Fig. 7 illustrates the obtained results. Initially, the presence of both light and TEMPO positively impacted  $\text{gC}_3\text{N}_4$ , resulting in a 100% conversion of HMF and a 39% selectivity for FFCA (Fig. 7a). However, it became evident that a significant amount of by-products (61%) was generated, implying that prolonged exposure of the catalyst to blue light facilitated secondary reactions. In the absence of the TEMPO mediator while keeping the presence of blue light (Fig. 7b), the conversion of HMF catalyzed by  $\text{gC}_3\text{N}_4$  decreased by half (50%). Additionally, a shift in the reaction selectivity was observed, enabling the observation of DFF formation (19%). Significant changes in conversion and selectivity values were not observed for the palladium modified carbon nitride sample ( $1\% \text{Pd/gC}_3\text{N}_4$ ). In addition, as expected, heterogenous catalysts were active only



Fig. 5 Laccase-catalysed redox cycles for substrate oxidation in a chemical mediator (TEMPO) presence.<sup>14,35</sup>





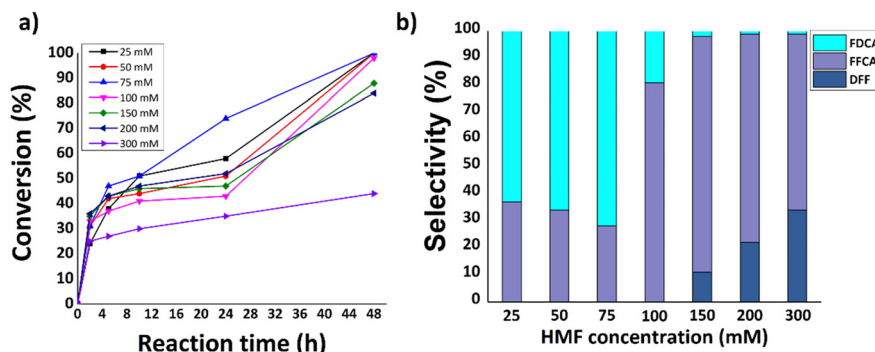


Fig. 6 Effect of HMF concentration (25, 50, 75, 100, 150, 200, and 300 mM, respectively) on the oxidation of HMF by LacTV-TEMPO system. (a) Conversion and (b) selectivity. Reaction condition: HMF (25–300 mM), TEMPO (0.3 equivalents), LacTV (5 U), reaction time (48 h), 30 °C and 300 rpm.

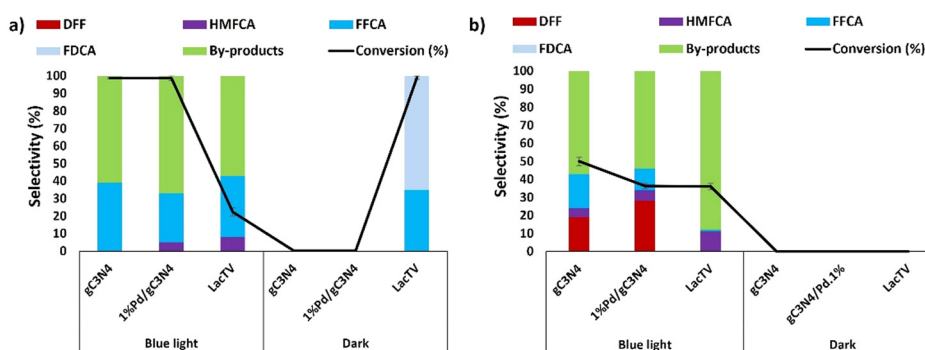


Fig. 7 Oxidation of HMF by LacTV,  $gC_3N_4$ , and 1%Pd/ $gC_3N_4$  in (a) TEMPO-mediated and (b) without TEMPO, in the presence and absence of blue light. Compounds: 2,5-furandicarboxaldehyde (DFF); 5-formyl-2-furoic acid (FFCA); 2,5-furandicarboxylic acid (FDCA) and 5-hydroxymethyl-2-furancarboxylic acid (HMFCFA); catalyst:  $gC_3N_4$  (graphitic carbon nitride), 1%Pd/ $gC_3N_4$  (graphitic carbon nitride with 1% palladium) and LacTV (free laccase from *Trametes versicolor*). Conditions: HMF (75 mM), TEMPO (0.3 equivalents), chemical catalyst (10 mg), LacTV (5U), citrate buffer (pH 6.0, 75 mM), reaction time (24 h), 400 rpm at 30 °C (dark) and blue light (460 nm).

in blue light (Fig. 7a and b), as no conversion was observed without the presence of light.

The  $gC_3N_4$  has an energy bandgap, known as the empty region, that extends from the top of the filled valence band (VB) to the bottom of the empty conduction band (CB). When the absorption of a photon with energy equal to or greater than the energy gap occurs, this results in the excitation of an electron from the VB to the CB, leaving behind an empty state, which constitutes a positive hole.<sup>38</sup> Once spatially separated, the charge carriers in the excited states, which migrated to the  $gC_3N_4$  surface, play a fundamental role in initiating the reduction and oxidation processes for the photocatalytic conversion of the reactant molecules.<sup>39</sup> In this context, the primary function of  $gC_3N_4$  is to absorb light, generate electron-hole pairs, and direct them to its surface or a co-catalyst, such as TEMPO. However,  $gC_3N_4$  is chemically active only when the electron-hole pair generated by photocatalysis is consumed instantly, avoiding recombination that would occur in fractions of nanoseconds.<sup>36,37</sup> In this context, Xu and co-workers<sup>7</sup> reported a study of the photocatalytic oxidation of HMF in the presence of cobalt thioporphyrine (CoPz) dis-

persed in  $gC_3N_4$  (CoPz/ $gC_3N_4$ ) with a high HMF conversion of 83.2% and an excellent FDCA selectivity of 98.1% under 400 nm wavelength irradiation. Furthermore, they highlighted the importance of singlet oxygen generated from the activation of molecular oxygen by photocatalysts in the selectivity of the reaction due to its capacity for the selective oxidation of HMF to FDCA, suggesting that the strong interaction between CoPz and  $gC_3N_4$  in the CoPz/ $gC_3N_4$  catalyst deactivated the generation of hydroxyl radical by  $gC_3N_4$  and promoted the generation of singlet oxygens at the CoPz sites, significantly improving the catalytic performance.<sup>7</sup> On the other hand, laccases are metalloenzymes known for their intriguing absorption properties. These properties can be used to enhance the oxidation of organic substrates through a photo-laccase system using visible light irradiation.<sup>40</sup> However, it is worth highlighting that under the conditions investigated, blue light in the LacTV-TEMPO system resulted in a decrease in conversion and the absence of the TEMPO mediator. On the contrary, in the absence of blue light, the LacTV-TEMPO system has a conversion of 100% and a selectivity for FDCA of 52%, as already seen in previous investigations in this study (Fig. 7a).



Considering the results obtained,  $g\text{-C}_3\text{N}_4$ ,  $1\%\text{Pd}/g\text{C}_3\text{N}_4$ , and  $\text{LacTV-TEMPO}$  were selected as catalysts for the oxidation of HMF, employing both photochemical and enzymatic processes within a modular flow chemical platform of continuous stirred tank reactors (CSTR).

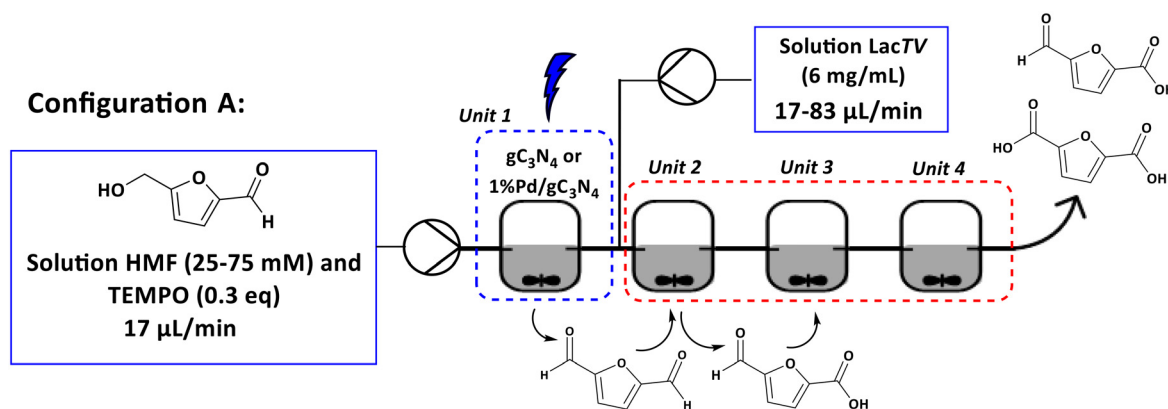
### Optimization of the oxidation HMF using a continuous stirred-tank reactor (CSTR) in a photochemical and enzymatic cascade

The next objective was to create a cascade process involving photocatalytic and enzymatic reactions using four Continuous Stirred Tank Reactor (CSTR) units. Two configurations (see configurations A and B, Fig. 8 and 9) were implemented. In the configuration A, a solution containing HMF was introduced into unit 1, which contained the photocatalyst and was exposed to blue light (460 nm). In the unit 2, a solution containing laccase was introduced. This enabled mixing the solu-

tion of HMF/products and laccase in unit 2, which proceeded then to units 3 and 4, where only agitation was applied. Based on the results obtained exclusively for unit 1 (configuration A – unit 1), a maximum conversion of 26% for  $1\%\text{Pd}/g\text{C}_3\text{N}_4$  (25 mM, 2 h) was observed and a selectivity of 72% to DFF (see ESI – Table S.1†).

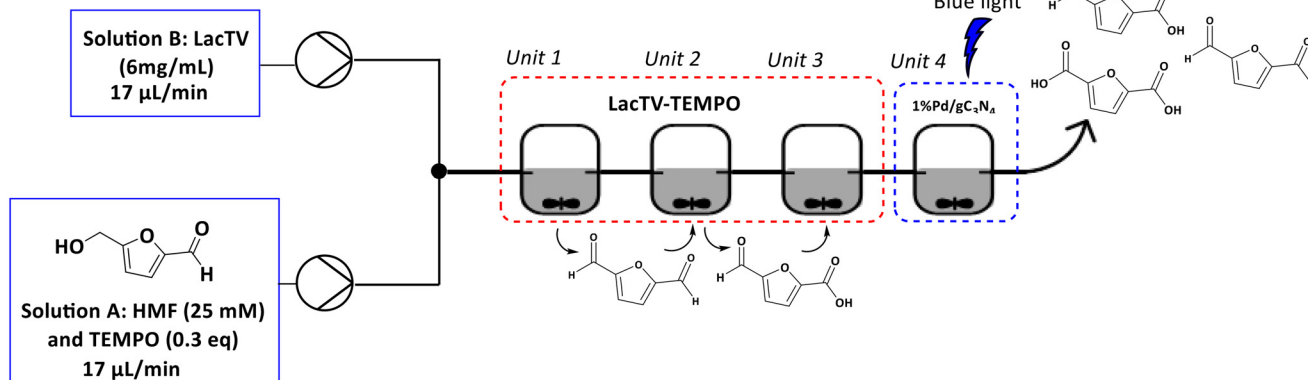
Furthermore, it was noted that an increase in the concentration of the HMF solution resulted in a reduction in conversion. For the system containing only the enzyme solution (configuration A – units 2–4), the increase in concentration had little influence on the conversion. However, a significant change in the selectivity of the reaction was observed, with FFCA being the main product.

Table 2 summarizes the results achieved in the oxidation of HMF in the configuration A using all units in sequence. The collaborative effect of the cascade reaction between the  $1\%\text{Pd}/g\text{C}_3\text{N}_4$  photocatalyst in the presence of blue light and free



**Fig. 8** Configuration proposal for HMF oxidation in cascade continuous stirred tank reactors (CSTR). HMF solution (25–75 mM, TEMPO 0.3 equivalents, citrate buffer pH 6.0 (75 mM));  $g\text{C}_3\text{N}_4$  or  $1\%\text{Pd}/g\text{C}_3\text{N}_4$  (unit 1)(10 mg) in the presence of blue light (460 nm – unit 1); LacTV solution (laccase from *Trametes versicolor*, 6 mg mL<sup>-1</sup>, citrate buffer pH 6.0 (75 mM)); flow unit 1 (17 µL min<sup>-1</sup>) under all conditions; flow units 2, 3 and 4 (17–83 µL min<sup>-1</sup>); 30 °C (units 2, 3 and 4) at 350 rpm.

### Configuration B:



**Fig. 9** Configuration proposal for HMF oxidation in cascade continuous stirred tank reactors (CSTR). Solution A: HMF solution (25 mM, TEMPO 0.3 equivalents, citrate buffer pH 6.0 (75 mM)) and constant flow (17 µL min<sup>-1</sup>); solution B: LacTV (laccase from *Trametes versicolor* (6 mg mL<sup>-1</sup>), citrate buffer pH 6.0 (75 mM)); constant flow (17 µL min<sup>-1</sup>) and  $1\%\text{Pd}/g\text{C}_3\text{N}_4$  (10 mg) in the presence of blue light (460 nm – unit 4); 30 °C (units 1, 2 and 3) at 350 rpm.



**Table 2** Results of HMF oxidation in cascade reaction using all units in sequence (configuration A, Fig. 8)

Entry	Photocatalyst	Total time (h)	Conversion (%)	Yield (%)				
				DFE	HMFCFA	FFCA	FDCA	By-products
1	gC <sub>3</sub> N <sub>4</sub>	3	77	5	0	62	7	2
2		4	96	3	0	75	16	2
3		5	100	6	0	73	19	2
4	1%Pd/gC <sub>3</sub> N <sub>4</sub>	3	100	5	0	76	17	2
5		4	100	4	0	72	21	3
6		5	100	1	0	67	31	1

Condition: initial HMF concentration (25 mM, 17  $\mu\text{L min}^{-1}$ , unit 1); TEMPO (0.3 equivalent); citrate buffer pH 6.0 (75 mM); 30 °C (units 2–4); 500 rpm; reaction time (3–5 h); g-C<sub>3</sub>N<sub>4</sub> and 1%Pd/gC<sub>3</sub>N<sub>4</sub> (10 mg – unit 1); and LacTV (6 mg mL<sup>-1</sup>, 33–100  $\mu\text{L min}^{-1}$ , units 2–4). Results only with gC<sub>3</sub>N<sub>4</sub> and 1%Pd/gC<sub>3</sub>N<sub>4</sub> (see ESI – Table S.1†).

laccase contributes to accelerating the conversion of the starting material in all demonstrated conditions, reaching 100% in 3 h of reaction. Furthermore, a maximum yield of 76% for FFCA in 3 h and 31% for FDCA in a total time of 5 h were achieved. Productivity calculations were performed to compare the cascade and batch reaction results. The cascade reaction exhibited a productivity of 3.44 mg of FDCA per min per mg LacTV. In comparison, the batch reaction produced a substantially lower productivity of 0.087 mg of FDCA per min per mg LacTV. The results indicate a significant advantage in favor of the cascade reaction, with an almost 40-fold increase yield compared to the batch system.

In configuration B, a T mixer was initially employed to mix solutions A and B. The resulting mixture then progressed through units 1, 2, and 3, where only stirring was applied. Subsequently, in unit 4, 1%Pd/gC<sub>3</sub>N<sub>4</sub> was present under blue light irradiation (460 nm). A 96% conversion was achieved for a total time of 5 hours. The selectivity observed was 66% for FFCA, 25% for FDCA, and 5% for DFE, with simultaneous formation of by-products. These results were similar to those found using configuration A.

## Experimental

### Chemicals

Laccases from *Trametes versicolor*, *Aspergillus* spp. and *Pseudomonas cepacea*. Albumin bovine serum (BSA), 2,2'-azino-di-(3-ethylbenzthiazoline sulfonic acid) (ABTS), 2,2,6,6-tetramethylpiperidine 1-oxyl, 2,2,6,6-tetramethyl-1-piperidinyloxy, free radical (TEMPO) (>98%), 2,5-diformylfuran (DFE), 5-hydroxymethyl-2-furancarboxylic acid (HMFCFA), 5-formyl-2-furancarboxylic acid (FFCA), 2,5-furandicarboxylic acid (FDCA) and 5-hydroxymethyl-furfural (HMF) were purchased from Sigma-Aldrich®. All other reagents used were of analytical grade. Graphitic carbon nitride (g-C<sub>3</sub>N<sub>4</sub>) and Pd modified (1%Pd/gC<sub>3</sub>N<sub>4</sub>) materials were synthesized as described in.<sup>41</sup> Details are also given in ESI.†

### Methods

**Determination of protein concentration.** The concentration of proteins from the enzyme extract of free laccase and super-

natants during the immobilization process was carried out according to the method of Bradford, where the protein content was estimated by the average of a calibration curve obtained using albumin bovine serum (BSA) as a standard<sup>42</sup> (see ESI – Fig. S.4†).

**Assessment of laccase activity.** A solution containing laccase was added to an Eppendorf tube containing 2.0 mL ABTS (25 mM) in phosphate buffer (pH 4.5) and then reacted at 30 °C and 200 rpm. Laccase activity was determined by monitoring the oxidation ABTS to ABTS<sup>•+</sup> ratio at 420 nm using a ThermoScientific™ GENESYS™ 150 UV-visible Spectrophotometer.<sup>43</sup> Each test was performed in a total volume of 2 mL at 30 °C. For free enzyme, 5 mg of laccase was added to 2 mL of ABTS solution (0.5 mM ABTS in pH 4.5 phosphate buffer solution) per 3 min. The reaction was quenched with a concentrated acidic hydrochloric solution. For biocatalytic particles, 10 mg of laccase-immobilized were dispersed in 2 mL of ABTS solution per 20 min. Prior to UV measurements, the solution was quickly filtered through a 0.1 mm Millipore syringe filter to remove biocatalytic particles. O absorbance was measured once per minute. One unit (U) of the laccase activity was defined as the amount of laccase forming 1  $\mu\text{mol}$  of ABTS<sup>•+</sup> per minute and could be calculated by the following equation:

$$\text{Laccase activity (A)} (\text{U m}^{-1}) = \frac{A \times 10^6 \times V}{\epsilon \times t \times m}$$

where A is the absorbance of ABTS<sup>•+</sup> at 420 nm ( $\epsilon$  is the molar extinction coefficient of radical cation ABTS<sup>•+</sup> at 420 nm = 36 000 L mol<sup>-1</sup> × cm); V represents the total volume of the reaction (L); t is the reaction time (min); 10<sup>6</sup> is the conversion factor from M to  $\mu\text{M}$ ; m is the total weight of the biocatalyst (mg) (see ESI – Fig. S.5 and 6†).

**General procedure for the laccase-mediated oxidation of HMF in batch.** A LightSyn Illumin8® reactor from ASYNT was used for reaction performed in batch. A solution of HMF (25–300 mM, 3 mL) in different buffers (pH 4.5–7.0) and TEMPO (0.3 equivalents) was added to an air-opened reaction tube. The reaction mixture was stirred magnetically for a few minutes to dissolve all the reactants, and then, the enzyme (5 U) or photocatalyst (gC<sub>3</sub>N<sub>4</sub> and 1%Pd/gC<sub>3</sub>N<sub>4</sub> – 20 mg) was





added. The mixture was stirred magnetically (300 rpm) for 48 h at controlled temperature (30 °C).

#### In CSTR

*Set-up A.* A *f*Reactor® from ASYNT was used for reaction performed in flow. A solution of HMF (25 and 75 mM, 10 mL) was prepared with citrate buffer pH 6.0 (75 mM) and TEMPO (0.3 equivalents). The solution was pumped into unit 1, which contained the photocatalyst. After 2 h of residence time, the reaction mixture entered unit 2, containing the enzyme solution, following the route to units 3 and 4, which were used only to increase the residence time (1–3 h, respectively), as shown in Fig. 8.

*Set-up B.* Solution A was prepared containing HMF (25 mM, 10 mL) with citrate buffer pH 6.0 (75 mM) and TEMPO (0.3 equivalents). Solution B with *LacTV* (6 mg mL<sup>-1</sup>) was prepared in parallel. Both solutions were previously pumped into a T-type mixer, from where they went to units 1, 2, and 3. After this step, the reaction mixture went to unit 4, which contained the 1%Pd/gC<sub>3</sub>N<sub>4</sub> photocatalyst in the presence of blue light, as indicated in Fig. 9.

#### Quantification of HMF, DFF, FFCA, HMFCA and FDCA

Samples were withdrawn at a specified time from the reaction and diluted 10 times by deionized water/sulfuric acid (5 mM). Samples containing products and not converted HMF were analyzed by high-performance liquid chromatography (HPLC) using a ThermoScientific Vanquish with a UV detector at 265 nm. A BioRad Aminex HPX-87H-organic acids column was used at 30 °C in isocratic elution mode (0.6 mL min<sup>-1</sup>) with a 5 mM L<sup>-1</sup> H<sub>2</sub>SO<sub>4</sub> solution as the mobile phase.

HMF, DFF, FFCA, HMFCA, and FDCA (Sigma ALDRICH, US) were used as standards to build the calibration curves (see ESI – Fig. S.7–15†).

## Conclusion

In conclusion, this study delved into the intricate dynamics of the oxidation of 5-hydroxymethylfurfural (HMF) to yield valuable products such as 2,5-furandicarboxaldehyde (DFF), 5-formyl-2-furancarboxylic acid (FFCA), and 2,5-furandicarboxylic acid (FDCA) through (photo)chemical and enzymatic catalysis cascade. Laccases from diverse sources were studied, with *Trametes versicolor* laccase (*LacTV*) emerging as the most efficient catalyst, showcasing complete HMF conversion under specific pH conditions. The elucidated reaction mechanisms unveiled a preference for the primary alcohol oxidation pathway, culminating in the formation of DFF and subsequent conversion to FFCA and FDCA. The investigation into substrate concentration unveiled optimal HMF conversion at lower concentrations (<100 mM), with diminished performance observed at higher concentrations (>100 mM). The study also explored the influence of blue light (430 nm) on the reaction, revealing its critical role for gC<sub>3</sub>N<sub>4</sub>-based catalysts and a contrasting negative effect for *LacTV*. The introduction of a modular flow chemical platform in a cascade configuration

marked an innovative approach for optimizing HMF oxidation. This implementation resulted in an impressive 40-fold increase in productivity compared to traditional batch systems, signifying significant progress in advancing green chemistry and sustainable chemical synthesis. The results offer a promising avenue for developing a more effective and selective process for producing valuable products from HMF at near ambient conditions. Looking ahead, it is suggested to explore the immobilization of laccase, aiming to facilitate biocatalyst recovery and unlocking additional benefits associated with the use of immobilized enzymes in future studies.

## Conflicts of interest

There are no conflicts to declare.

## Acknowledgements

Authors thank Fundação Carlos Chagas Filho de Amparo à Pesquisa do Estado do Rio de Janeiro for Jovem Cientista do Nosso Estado Grant Number: E-203.267/2017, Conselho Nacional de Desenvolvimento Científico e Tecnológico (BR) for Universal Grant Number 429974/2018-3, Centrale Lille, the CNRS, and Lille University as well as the Centrale Initiative Foundation, for their financial contribution. LIA CNRS France-Brazil's "Energy & Environment" and Métropole Européen de Lille (MEL) for the "CatBioInnov" project are also acknowledged.

## References

- R. J. Van Putten, J. C. Van Der Waal, E. De Jong, C. B. Rasrendra, H. J. Heeres and J. G. De Vries, *Chem. Rev.*, 2013, **113**, 1499–1597.
- D. A. Giannakoudakis, V. Nair, A. Khan, E. A. Deliyanni, J. C. Colmenares and K. S. Triantafyllidis, *Appl. Catal., B*, 2019, **256**, 117803.
- I. Itabaiana Jr, M. A. Do Nascimento, R. O. M. A. De Souza, A. Dufour and R. Wojcieszak, *Green Chem.*, 2020, **22**, 5859–5880.
- P. Zhou and Z. Zhang, *Catal. Sci. Technol.*, 2016, **6**, 3694–3712.
- K. I. Galkin and V. P. Ananikov, *ChemSusChem*, 2019, **12**, 2976–2982.
- S. Chen, R. Wojcieszak, F. Dumeignil, E. Marceau and S. Royer, *Chem. Rev.*, 2018, **118**, 11023–11117.
- S. Xu, P. Zhou, Z. Zhang, C. Yang, B. Zhang, K. Deng, S. Bottle and H. Zhu, *J. Am. Chem. Soc.*, 2017, **139**, 14775–14782.
- Y. Xu, X. Jia, J. Ma, J. Gao, F. Xia, X. Li and J. Xu, *ACS Sustainable Chem. Eng.*, 2018, **6**, 2888–2892.
- D. Gao, F. Han, G. I. N. Waterhouse, Y. Li and L. Zhang, *Catal. Commun.*, 2023, **173**, 106561.



- 10 M. Sayed, S. H. Pyo, N. Rehnberg and R. Hatti-Kaul, *ACS Sustainable Chem. Eng.*, 2019, **7**, 4406–4413.
- 11 Q. Zhu, Y. Zhuang, H. Zhao, P. Zhan, C. Ren, C. Su, W. Ren, J. Zhang, D. Cai and P. Qin, *Chin. J. Chem. Eng.*, 2023, **54**, 180–191.
- 12 M. Braun and M. Antonietti, *Green Chem.*, 2017, **19**, 3813–3819.
- 13 B. Liu, Y. Ren and Z. Zhang, *Green Chem.*, 2015, **17**, 1610–1617.
- 14 F. D'Acunzo, P. Baiocco, M. Fabbrini, C. Galli and P. Gentili, *Eur. J. Org. Chem.*, 2002, **2002**, 4195–4201.
- 15 W. Huang, W. Zhang, Y. Gan, J. Yang and S. Zhang, *Crit. Rev. Environ. Sci. Technol.*, 2022, **52**, 1282–1324.
- 16 W. Zhou, W. Zhang and Y. Cai, *Chem. Eng. J.*, 2021, **403**, 126272.
- 17 S. Riva, *Trends Biotechnol.*, 2006, **24**, 219–226.
- 18 L. Arregui, M. Ayala, X. Gómez-Gil, G. Gutiérrez-Soto, C. E. Hernández-Luna, M. H. De Los Santos, L. Levin, A. Rojo-Domínguez, D. Romero-Martínez, M. C. N. Saparrat, M. A. Trujillo-Roldán and N. A. Valdez-Cruz, *Microb. Cell Fact.*, 2019, **18**, 200.
- 19 F. Koopman, N. Wierckx, J. H. De Winde and H. J. Ruijsenaars, *Proc. Natl. Acad. Sci. U. S. A.*, 2010, **107**, 4919–4924.
- 20 M. Krystof, M. Pérez-Sánchez and P. D. De María, *ChemSusChem*, 2013, **6**, 826–830.
- 21 J. Carro, P. Ferreira, L. Rodríguez, A. Prieto, A. Serrano, B. Balcells, A. Ardá, J. Jiménez-Barbero, A. Gutiérrez, R. Ullrich, M. Hofrichter and A. T. Martínez, *FEBS J.*, 2015, **282**, 3218–3229.
- 22 W. P. Dijkman and M. W. Fraaije, *Appl. Environ. Microbiol.*, 2014, **80**, 1082–1090.
- 23 S. Cao and J. Yu, *J. Phys. Chem. Lett.*, 2014, **5**, 2101–2107.
- 24 C. Zhang, X. Chang, L. Zhu, Q. Xing, S. You, W. Qi, R. Su and Z. He, *Int. J. Biol. Macromol.*, 2019, **128**, 132–139.
- 25 N. Cascelli, V. Lettera, G. Sannia, V. Gotor-Fernández and I. Lavandera, *ChemSusChem*, 2023, **16**, e202300226.
- 26 A. D. Cheng, M. H. Zong, G. H. Lu and N. Li, *Adv. Sustainable Syst.*, 2021, **5**, 2000297.
- 27 I. Bassanini, E. E. Ferrandi, S. Riva and D. Monti, *Catalysts*, 2021, **11**, 1–30.
- 28 W. P. Dijkman, D. E. Groothuis and M. W. Fraaije, *Angew. Chem., Int. Ed.*, 2014, **53**, 6515–6518.
- 29 Z. Y. Yang, M. Wen, M. H. Zong and N. Li, *Catal. Commun.*, 2020, **139**, 105979.
- 30 Y. Pecker and J. E. Meany, *J. Phys. Chem.*, 1967, **71**, 3113–3120.
- 31 R. A. McClelland and M. Coe, *J. Am. Chem. Soc.*, 1983, **105**, 2718–2725.
- 32 H. X. Zhou and X. Pang, *Chem. Rev.*, 2018, **118**, 1691–1741.
- 33 A. Schön, S. Y. Lam and E. Freire, *Future Med. Chem.*, 2011, **3**, 1129–1137.
- 34 J. C. Stevens, D. W. Rodgers, C. Dumon and J. Shi, *Front. Energy Res.*, 2020, **8**, 00158.
- 35 M. Fabbrini, C. Galli, P. Gentili and D. Macchitella, *Tetrahedron Lett.*, 2001, **42**, 7551–7553.
- 36 S. D. Perera, R. G. Mariano, K. Vu, N. Nour, O. Seitz, Y. Chabal and K. J. Balkus, *ACS Catal.*, 2012, **2**, 949–956.
- 37 K. Woan, G. Pyrgiotakis and W. Sigmund, *Adv. Mater.*, 2009, **21**, 2233–2239.
- 38 W. J. Ong, L. L. Tan, Y. H. Ng, S. T. Yong and S. P. Chai, *Chem. Rev.*, 2016, **116**, 7159–7329.
- 39 S. N. Habisreutinger, L. Schmidt-Mende and J. K. Stolarczyk, *Angew. Chem., Int. Ed.*, 2013, **52**, 7372–7408.
- 40 V. Giraldi, M. Marchini, M. Di Giosia, A. Gualandi, M. Cirillo, M. Calvaresi, P. Ceroni, D. Giacomini and P. G. Cozzi, *New J. Chem.*, 2022, **46**, 8662–8668.
- 41 E. Alwin, R. Wojcieszak, K. Kočí, M. Edelmannová, M. Zieliński, A. Suchora, T. Pędziński and M. Pietrowski, *Materials*, 2022, **15**, 710.
- 42 M. M. Bradford, *Anal. Biochem.*, 1976, **72**, 248–254.
- 43 H. Shan, X. Wang, Y. Ge and Z. Li, *J. Hazard. Mater.*, 2022, **423**, 127107.

